Available online at www.sciencedirect.com

ScienceDirect

IFAC Papers Online CONFERENCE PAPER ARCHIVE

IFAC PapersOnLine 55-20 (2022) 391–396

Macroscopic Modeling of Intracellular Trehalose Concentration in *Saccharomyces cerevisiae* Fed-batch Cultures ⋆

Antoine Huet * **Mihaela Sbarciog** * **Philippe Bogaerts** *

* *3BIO-BioControl, Université Libre de Bruxelles, CP 165/61, 50, Av. F.-D. Roosevelt, B-1050 Brussels, Belgium (e-mail: antoine.huet@ulb.be; mihaela.iuliana.sbarciog@ulb.be; philippe.bogaerts@ulb.be).*

Abstract: This paper describes the extension of a baker's yeast growth model to account for the intracellular trehalose storage and mobilization. Trehalose is a reserve carbohydrate that is accumulated and converted back to intracellular glucose when the yeast cells face certain stresses. This is modeled by a new macroscopic reaction, which is coupled to an existing macroscopic reaction scheme describing the coordinated uptake of glucose and ammonium by the yeast cells. The dynamics of the trehalose concentration is described by a delay differential equation as the available experimental data used to fit the model exhibits a time-delayed correlation between trehalose storage and glucose uptake as well as a time-delayed correlation between trehalose mobilization and ethanol respiration phases. The proposed extension contains 6 parameters of which 5 are estimated via nonlinear least squares identification. The proposed model predicts accurately the dynamics of trehalose storage and mobilization and can be used to optimize the intracellular trehalose accumulation in *Saccharomyces cerevisiae*, which is valuable for obtaining reinforced yeast cells, able to better withstand drying operations.

Keywords: Saccharomyces cerevisiae, dynamical model, overflow metabolism, trehalose, stress protection, delay differential equations

1. INTRODUCTION

Saccharomyces cerevisiae, also known as baker's yeast, is one of the most widely used and researched microorganisms. It usually serves as a model for eukaryotic cells. Industrial uses of yeast fed-batch culture ranges from the food and alcoholic beverages to the production of biofuels and chemicals such as bioethanol (Parapouli et al., 2020).

Improving efficiency in industry is an everlasting objective. In the agro-food industry, it is essential to reach high cell viability rate when forming dry yeast. However, during the various processes, cells encounter several stress-inducing environments: the culture medium can be hypertonic and leads to osmotic stress, high level of ethanol is toxic for the cells, and processing, such as yeast drying, subjects cells to high temperature variations. All these stresses increase the mortality rate of the yeast cells. It has been proven (Ohtake and Wang, 2011) that the intracellular accumulation of trehalose, a sugar naturally synthesized within insects, plants and yeasts, rises the resistance to these stresses and therefore the viability of yeast cells in industrial bioprocesses (Tapia and Koshland, 2014; Saini et al., 2018).

Aside of being a highly efficient protectant that enhances the yeast cells resistance in hostile conditions, trehalose has many utilizations in practice such as stabilizer in reagents and bioproducts (enzymes, proteins, biomasses), preservative for food, component in cosmetics, cryoprotectant for preserving cells in medicine and microbiology (Du and Zhao, 2012). Hence, a high trehalose production rate is desired, which can be achieved by process optimization. To avoid long lasting and expensive experimental work, process optimization is performed based on a process model (Richelle and Bogaerts, 2014). Models that predict trehalose formation are scarce. Moreover, they are either based on the cell metabolic network rather than describing the population dynamics or consider that glucose is the only nutrient that the cells need for growth (Voit, 2003; Aranda et al., 2004).

This study proposes an extension to a macroscopic model describing fed-batch baker's yeast growth (Richelle et al., 2014), to incorporate the trehalose dynamics.The resulting model includes overflow metabolism phenomena, coordinated uptake of glucose and nitrogen, and intracellular trehalose storage and mobilization for *S. cerevisiae* fed-batch cultures. The paper is organized as follows. Section 2 introduces the growth model with coordinated uptake of glucose and nitrogen, while Section 3 details the cell trehalose cycle, the macroscopic reaction added to the existing model and the storage and mobilization reaction rates. Parameter estimation from the available experimental database and model validation are discussed in Sec-

⋆ This research has been funded by the Wallonia Region (SPW Recherche) and supported by Wagralim, the agri-food innovation cluster in Wallonia Region, within the framework of the WA-SuNuP project.

10.1016/j.ifacol.2022.09.126

tion 4, while conclusions and possible model improvements are indicated in Section 5.

2. YEAST GROWTH MODEL WITH COORDINATED UPTAKE OF GLUCOSE AND AMMONIUM

One of the most renowned and accepted dynamical models able to reproduce overflow metabolism in *S. cerevisiae* cultures was proposed by Sonnleitner and Käppeli (1986). They introduced a maximum respiratory capacity by a simple mechanism with min-max non-linearities to model the overflow metabolism. The model considers only glucose uptake and has been widely used to simulate and optimize *S. cerevisiae* growth. However, it is well known that ammonium plays an important role in microorganisms growth and the activation of the cellular metabolism as it is a main component of proteins and nucleic acids. Hence, accurate predictions of yeast growth may be obtained only using a model which describes the coordinated uptake of carbon and nitrogen sources, such as the one proposed by Richelle et al. (2014). By the means of a new macroscopic reaction in addition of those presented by Sonnleitner and Käppeli (1986), Richelle et al. (2014) introduced the coordinated uptake of ammonium as well as an intracellular metabolite, α-ketoglutarate, that acts as an inhibitor of the fermentation. α-ketoglutarate is produced when biomass grows on glucose through fermentation and can be consumed along with ammonium. Considering fully aerobic conditions, the reaction network describing the process is given by:

$$\begin{aligned} G &\xrightarrow{r_1} k_1 X \\ G &\xrightarrow{r_2} k_2 X + k_4 E + k_7 A \\ E &\xrightarrow{r_3} k_3 X \\ N + A &\xrightarrow{r_4} k_8 X \end{aligned} \tag{1}$$

In (1), X, G, N, E and A respectively denote the biomass concentration (g/L), extracellular glucose concentration (g/L), ammonium concentration (g/L), ethanol concentration (g/L) and intracellular α-ketoglutarate concentration (g/gX). $k_1 \dots k_8$ represent the pseudo-stoichiometric coefficients. The reactions included in the network (1) express: i) biomass growth on glucose through respiration; ii) biomass growth on glucose through fermentation, with ethanol production and α-ketoglutarate accumulation; iii) biomass growth on ethanol through respiration, which is only possible if the global glucose uptake is inferior to the maximum respiratory capacity and occurs only in the presence of ethanol; iv) formation of biomass on ammonium as well as coordinated consumption of α-ketoglutarate, therefore boosting the fermentation as α-ketoglutarate is considered an inhibitor of the fermentation.

For a fed-batch process, which is the common way of growing yeast in industry, the system dynamics are described by the mass balance equations (2), where F is the feed flow rate, V is the culture volume, G^{in} and N^{in} are respectively the glucose concentration and ammonium concentration in the feed and r_i, $i = 1 \dots 4$ are the reaction rates. The specific rate of respiration, the glucose uptake rate and ammonium uptake rate are given by (3), while the overflow metabolism is expressed similarly as in (Sonnleitner and Käppeli, 1986) through the kinetic rates (4).

$$\begin{aligned} \frac{dX}{dt} &= k_1 r_1 X + k_2 r_2 X + k_3 r_3 X + k_8 r_4 X - \frac{F}{V} X \\ \frac{dG}{dt} &= -r_G X + \frac{F}{V}\left(G^{in} - G\right) \\ \frac{dN}{dt} &= -r_4 X + \frac{F}{V}\left(N^{in} - N\right) \\ \frac{dE}{dt} &= k_4 r_2 X - r_3 X - \frac{F}{V} E \\ \frac{dA}{dt} &= k_7 r_2 - r_4 - A\left(k_1 r_1 + k_2 r_2 + k_3 r_3 + k_8 r_4\right) \\ \frac{dV}{dt} &= F \end{aligned} \tag{2}$$

$$\begin{aligned} r_O &= \alpha \frac{K_I}{E + K_I} \\ r_G &= \mu_{Gmax} \frac{G}{G + K_G} \frac{K_{IA}}{(AX) + K_{IA}} \\ r_N &= \mu_{Nmax} \frac{N}{N + K_N} \frac{(AX)}{(AX) + K_A} \frac{K_{IA2}}{(AX) + K_{IA2}} \end{aligned} \tag{3}$$

$$\begin{aligned} r_1 &= \min\left(r_G, r_O\right) \\ r_2 &= \max\left(0, r_G - r_O\right) \\ r_3 &= \max\left(0, \left(r_O - r_G\right) \frac{E}{E + K_E}\right) \\ r_4 &= r_N \end{aligned} \tag{4}$$

The model parameters (Richelle et al., 2014) are presented in Table 1. These parameters have been identified from experimental data. The experimental database contains also measurements of the intracellular trehalose concentration, which will be used in the next sections for model extension.

Table 1. Model parameters

Name	Value	Units	Name	Value	Units
k_1	0.5998	gX/gG	μ_{Nmax}	1.1903	gN/gX/h
k_2	0.0662	gX/gG	K_G	0.1524	gG/L
k_3	0.9386	gX/gE	K_I	3.1817	gE/L
k_4	0.2452	gE/gG	K_E	0.1	gE/L
k_7	0.2389	gA/gG	K_N	2.9370	gN/L
k_8	1.0150	gX/gN	K_A	9.0014	gA/L
α	0.4445	gG/gX/h	K_{IA}	5.5981	gA/L
μ_{Gmax}	2.5364	gG/gX/h	K_{IA2}	5.7737	gA/L

3. TREHALOSE STORAGE AND MOBILIZATION

3.1 Biological Insight

Trehalose is a disaccharide formed from two glucose molecules according to a pathway revealed by Cabib and Leloir (1958). As stated by Smallbone et al. (2011), the trehalose pathway in yeast consists of a small number of reactions, which occur in a metabolic cycle. These reactions are governed by a complex regulatory system, including various activation and inhibition signals, which makes the experimental study of pathway operation difficult. The trehalose cycle (Smallbone et al., 2011; Voit, 2003) comprises: the conversion of glucose into glucose 6-phosphate (G6P); the formation of trehalose 6-phosphate (T6P) from glucose 6-phosphate and uridine diphosphate glucose (UDPG); the conversion of trehalose 6-phosphate (T6P) into trehalose; the splitting of trehalose into two glucose molecules. This cycle is characterized by the reactions:

$$2G_{int} \longrightarrow G6P + UDPG \longrightarrow T6P \longrightarrow T \longrightarrow 2G_{int} \tag{5}$$

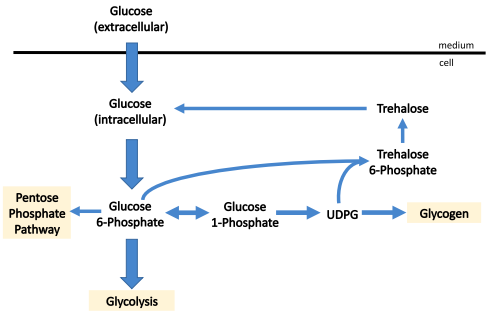

Fig. 1. Schematic representation of material flow in trehalose cycle in *S. cerevisiae* (Voit, 2003)

where G_{int} denotes the intracellular glucose and T denotes the intracellular trehalose. The trehalose cycle is illustrated in Figure 1 (Voit, 2003), where for simplicity only the flux of material is included while the activation and inhibition signals are discarded.

3.2 Model Rationales

The goal of this work is to identify a simple macroscopic model that relates trehalose dynamics to the yeast growth model (2). A model implementing cycle (5) will be fairly complex taking into account the various activation and inhibition terms and the number of components involved in the reactions. Moreover, its identification will be hampered by the lack of measurements, as the only intracellular measurement available is trehalose. Hence, the trehalose cycle is approximated in this work by a storage reaction, which relates the internal glucose to trehalose formation, and a mobilization reaction, which characterizes the conversion of trehalose to intracellular glucose:

$$G_{int} \underset{r_{mT}}{\overset{r_{sT}}{\rightleftharpoons}} \frac{1}{2}T \tag{6}$$

Note, however, that the internal glucose concentration is not measured and the reaction rates for storage and accumulation must be correlated to the available extracellular measurements. Opposite to the reaction scheme (1), which involves pseudo-stoichiometric coefficients, a direct stoichiometric coefficient is considered in (6), as one trehalose molecule is formed from two glucose molecules.

The proposed storage rate and mobilization rate are

$$r_{sT} = \mu_{sTmax} \cdot r_G\left(t-\tau_s\right) \cdot \frac{K_{IsN}}{N+K_{IsN}} \tag{7}$$

$$r_{mT} = \mu_{mTmax} \cdot r_3\left(t-\tau_m\right) \cdot \frac{T}{T+K_{mT}} \tag{8}$$

and the trehalose mass balance is given by

$$\frac{dT}{dt} = \frac{1}{2}r_{sT}X - \frac{1}{2}r_{mT}X - \frac{F}{V}T \tag{9}$$

In (7)-(9), T (g/L) denotes the product of intracellular trehalose (g/(g biomass)) and biomass concentration (g/L). This notation will be used in all further developments.

The structures of the storage and mobilization rates are chosen based on biological evidence and analysis of the available data sets. Trehalose is formed from intracellular glucose, whose availability is directly linked to the glucose uptake rate (r_G). However, the uptake of extracellular glucose does not imply the instantaneous increase of trehalose, as transport phenomena are involved, intracellular processes which are neither modeled nor fully understood occur, while the operational conditions greatly influence the cell cycle inducing stresses, which can trigger either carbohydrates storage or mobilization. The available data sets indicate a time-delayed correlation between trehalose storage and the global glucose uptake rate, hence, the term $r_G\left(t-\tau_s\right)$ is included in (7), where τ_s denotes the time delay for trehalose storage. On the other hand, trehalose is low (or zero) at high ammonium concentrations and its storage boosts when ammonium decreases to low quantities. Hence, the factor $\frac{K_{IsN}}{N+K_{IsN}}$ is included in the storage rate to account for ammonium inhibition.

Trehalose mobilization occurs when glucose is exhausted (or it is very low) and the culture is in the ethanol respiration phase. A similar time-delayed dependency between trehalose mobilization and ethanol respiration is observed in the experimental data, modeled by the term $r_3\left(t-\tau_m\right)$, where τ_m denotes the time delay for trehalose mobilization. Although no trehalose limitation has been noticed, the factor $\frac{T}{T+K_{mT}}$ is included in the mobilization rate to keep the model physical: no trehalose can be mobilized if it is not available. Therefore, the parameter K_{mT} is not identified from the available data but set to an arbitrarily small value ($K_{mT} = 0.01\text{gT/L}$).

To summarize, the proposed model for characterizing the trehalose dynamics consists of the delay differential equation (9), with the reaction rates (7)-(8) involving five parameters that need to be identified from the experimental data: two maximum specific rates μ_{sTmax} and μ_{mTmax}, two time delays τ_s and τ_m and the ammonium inhibition constant K_{IsN}. The model is simulated in MATLAB using the solver `dde23`.

4. PARAMETER ESTIMATION AND MODEL VALIDATION

The parameters of the trehalose accumulation and mobilization model are estimated from the experimental data acquired by Richelle et al. (2014). This experimental database consists of 4 fed-batch experiments that differ mainly at the level of the ammonium feeding concentration. The experiments last 21 hours and measurements are available at 15 or 16 time instants per experiment. These measurements include extracellular concentrations: biomass, glucose, ammonium, and ethanol, as well as intracellular trehalose concentration.

The parameters of the model extension (7)-(9) are identified using MATLAB `lsqnonlin` function, which applies the trust-region-reflective optimization algorithm to minimize a least-squares criterion. This criterion consists of the sum of squared differences between model predictions and the experimental values

$$SSE\left(\theta\right) = \sum_{j=1}^{n}\sum_{i=1}^{N_j}\left(\hat{y}_{ij}\left(\theta\right) - y_{ij}\right)^2 \tag{10}$$

where $\theta = [\,\mu_{sTmax}\ \mu_{mTmax}\ K_{IsN}\ \tau_s\ \tau_m\,]$ is the parameters vector, $\hat{y}_{ij}\left(\theta\right)$ represents the trehalose concentration

Table 2. Estimated parameters

Parameter**	Range of initialization	Set 1 Experiments 1-2-3-4	Set 2 Experiments 1-2-3	Set 3 Experiments 1-2-4	Set 4 Experiments 1-3-4	Set 5 Experiments 2-3-4	Variation coefficients*
μ_{sTmax}	0.01-0.1	0.0500	0.0419	0.0426	0.0607	0.0500	8.40
μ_{mTmax}	0.1-0.5	0.4796	0.3631	0.2995	0.3348	0.2296	16.00
K_{IsN}	0.01-0.1	0.3317	0.3291	0.4516	0.2528	0.2506	25.00
τ_s	5-10	6.080	6.1678	5.7859	7.1978	6.2154	0.0025
τ_m	1-5	3.3905	4.2764	1.4766	3.2149	2.7286	0.51
SSE*	/	0.7083	0.9131	0.8310	0.7638	0.7506	/

* calculated for Set 1 ** see units in Table 3

Table 3. Confidence intervals of the estimated parameters

Parameter	Set 1 Experiments 1-2-3-4	Set 2 Experiments 1-2-3	Set 3 Experiments 1-2-4	Set 4 Experiments 1-3-4	Set 5 Experiments 2-3-4	Units
μ_{sTmax}	[0.0416, 0.0584]	[0.0208, 0.0473]	[0.0337, 0.0514]	[0.0000, 0.0845]	[0.0427, 0.0654]	gT/gG
μ_{mTmax}	[0.3262, 0.6330]	[0.0114, 0.2709]	[0.0000, 0.6657]	[0.0233, 0.5545]	[0.0735, 1.0352]	gT/gE
K_{IsN}	[0.1658, 0.4976]	[0.0875, 0.6250]	[0.2194, 0.6839]	[0.0000, 0.8961]	[0.1374, 0.4792]	gN/L
τ_s	[6.0797, 6.0803]	[5.0853, 6.2727]	[5.7523, 5.8195]	[4.8016, 5.4277]	[6.2446, 6.4566]	h
τ_m	[3.3558, 3.4251]	[2.1127, 2.6372]	[1.4375, 1.5158]	[2.2977, 2.3178]	[3.2521, 3.2583]	h

predicted by the model (7)-(9) at the ith time instant in the jth experiment, y_{ij} is the measured trehalose concentration at the ith time instant in the jth experiment.

The hypothesis of a constant measurement error variance is made. Therefore, its unbiased estimate is calculated as

$$\hat{\sigma}^2 = \frac{SSE(\hat{\theta})}{N-p} \tag{11}$$

where $\hat{\sigma}^2$ denotes the estimated variance on the measurement error, $\hat{\theta}$ is the parameter set that minimizes criterion (10), $N = \sum_{j=1}^{n} N_j$ is the total number of trehalose measurements and p is the number of parameters. The sensitivity functions can be inferred from the Jacobian matrix (J) provided by the `lsqnonlin` solver. This matrix is used to compute a lower bound of the covariance matrix of the parameter estimation errors (S_d) based on the Fischer information matrix (F)

$$F = J^T \cdot J \qquad S_d = \hat{\sigma}^2 F^{-1} \tag{12}$$

The variance of each parameter is then obtained as

$$\sigma^2_{\theta_i} = S_{dii} \tag{13}$$

which leads to the 95% confidence intervals of the estimated parameters θ_i, with $i = 1 \dots 5$

$$CI_{\theta_i} = \theta_i \pm 2\sigma_{\theta_i} \tag{14}$$

Variation coefficients are also computed as

$$VC_{\theta_i} = \frac{\sigma_{\theta_i}}{\theta_i} \tag{15}$$

To avoid local minima and convergence problems, a multistart approach is used. For each parameter, pseudo-random values over given ranges were used for the initialization of the optimization algorithm. In total, 15 initializations were performed. The second column of Table 2 displays the ranges for parameters initialization. The set of parameters providing the lowest value of the cost function (10) was selected and reported in Table 2.

Several sets of parameters were estimated from different data sets. These data sets were built from the experimental database considering either the whole set of experimental data points (Set 1, comprising experiments 1 to 4) or a leave-one-out approach (Sets 2 to 5), in which the data points from one experiment are not used in the identification but are employed for cross validation. The identified sets of parameters are given in Table 2, while the confidence intervals calculated using the approach (11)-(14) are reported in Table 3. Figure 2 displays the experimental data (experiment 1) and the model predictions. The parameters estimated using the entire database (Set 1) are used for trehalose prediction. Figure 3 presents the direct validation (with Set 1) for each experiment, while Figure 4 shows the leave-one-out cross validation.

Comparing the two maximum rates, the largest uncertainty is observed for μ_{mTmax} (16% for μ_{mTmax} compared to 8.4% for μ_{sTmax}). This is caused by the fact that there are less instants in the four experiments in which there is trehalose mobilization compared to trehalose storage, which occurred more frequently.

The largest uncertainty is observed for K_{IsN} (25%). It is well known that environmental stress, such as low ammonium concentration, boosts trehalose accumulation in *S. cerevisiae*. It should be noted though that the ammonium concentration measurements are the ones with the highest standard variation in comparison to the signals range as seen in Figure 2.

The uncertainties for both τ_s and τ_m are very small (0.0025% and 0.51% respectively). This shows in both cases a clear time-delayed correlation between the kinetic rates of trehalose and the uptake of glucose as well as the respiration of ethanol. It is worthwhile noting that in comparison to other similar biological models (Amribt et al., 2013; Richelle et al., 2014), the variations for all parameters are in acceptable ranges and that they do not indicate the need for model reduction.

The 95% confidence intervals presented in Table 3 show that the results of parameter estimation with both direct validation and leave-one-out cross validation are quite similar. Moreover, the 5 sets of parameters lead to a sum of squared errors (SSE) of same order of magnitude (Table 2). This is of importance as the main difference between

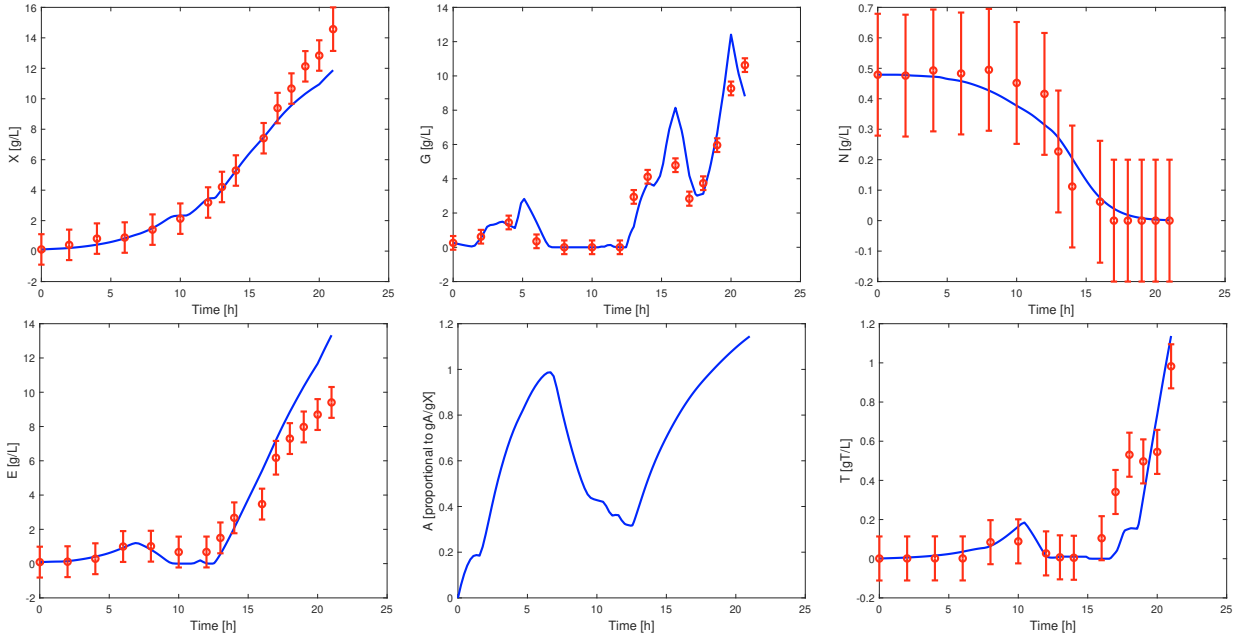

Fig. 2. Experiment 1: measurements (red dots) and model predictions (blue lines)

the four experiments is the ammonium concentration in the feeding medium. The predicted values are globally in good accordance with the experimental measurements and cross validation results are somewhat close to them. The trehalose predicted by the model using the parameters identified from Set 1 (direct validation) are presented in Figure 3. The transient behavior of trehalose is well captured for the four experiments. The final accumulation is well reproduced for experiment 4. However, there is an undershoot for experiment 2 and an overshoot for experiment 3. The final value for experiment 1 is closer to the experimental measurement and the second transient is reproduced in terms of trend but not with close values.

The trehalose predictions based on the sets of parameters identified from the leave-one-out approach (cross validation) are presented in Figure 4. In the case of experiment 1 (no ammonium in the feeding medium) and experiment 2 (high ammonium concentration in the feeding medium), the cross validation results are quite close to the direct validation ones. For experiment 3 (medium ammonium concentration in the feeding medium), the first transient almost disappears, and the model is not able to reproduce the first trehalose mobilization, resulting in a bit higher final overshoot than in direct validation. In the case of experiment 4, the simulation is quite close to the direct validation up till $t = 20$h, where trehalose storage diminishes and the prediction ends up in an underestimation of the measurement. Experiment 4 was performed with high ammonium concentration in the feeding medium during the first 15 hours and no ammonium feeding for the rest of the culture. This is the experiment in which the culture reaches the highest trehalose concentration out of the 4 experiments (1.3 g/L). By removing this experiment from the data set used for estimation, the model is not exposed during the identification to such high levels of trehalose concentration (second highest trehalose concentration is measured in experiment 1 with a concentration of 1 g/L). These observations highlight the importance of the experimental database used for parameter estimation, which must characterize the entire range of interest to allow the identification of a model able to accurately predict the process states. The model simulated with the parameters identified from Set 1 provides the best approximation of the fourth experiment. This is the experiment performed with the most suitable conditions for trehalose final accumulation.

5. CONCLUSION

In this study, an extension enabling trehalose concentration prediction was added to a validated macroscopic model for fed-batch cultures of *S. cerevisiae*. The model parameters were estimated from the available experimental database. The model predicts accurately the storage and mobilization of trehalose in *S. cerevisiae* for the operational conditions characterized by the available experimental database. The model may be improved if additional experimental data measured during trehalose mobilization phase is available. In a later stage, the model will be extended to include the dynamics of other reserve carbohydrates such as glycogen.

REFERENCES

Amribt, Z., Niu, H., and Bogaerts, Ph. (2013). Macroscopic modelling of overflow metabolism and model based optimization of hybridoma cell fed-batch cultures. *Biochem. Eng. J.*, 70, 196–209.

Aranda, J., Salgado, E., and Taillandier, P. (2004). Trehalose accumulation in *Saccharomyces cerevisiae* cells: experimental data and structured modeling. *Biochem. Eng. J.*, 17, 129–140.

Cabib, E. and Leloir, L. (1958). Biosynthesis of trehalose phosphate. *J. Biol. Chem.*, 231, 259–275.

Du, Y. and Zhao, Y. (2012). Optimization of fermentation conditions for trehalose production by a marine yeast. *Afr. J. Biotechnol.*, 11, 3352–3357.

Ohtake, S. and Wang, Y. (2011). Trehalose: current use and future applications. *J. Pharm. Sci.*, 101, 2020–2053.

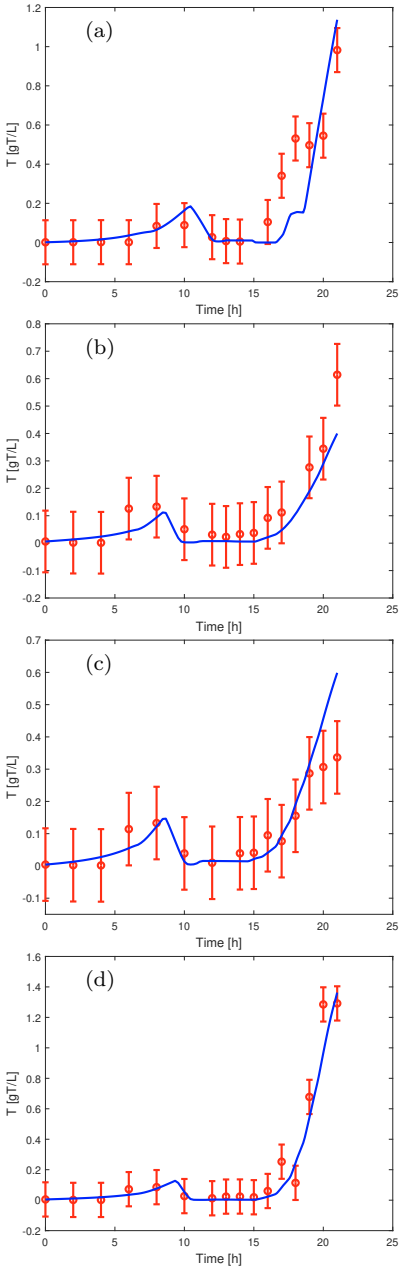

Fig. 3. Direct validation: predictions are obtained using the parameter set estimated from the entire experimental database (Set1).(a) Experiment 1, (b) Experiment 2, (c) Experiment 3, (d) Experiment 4

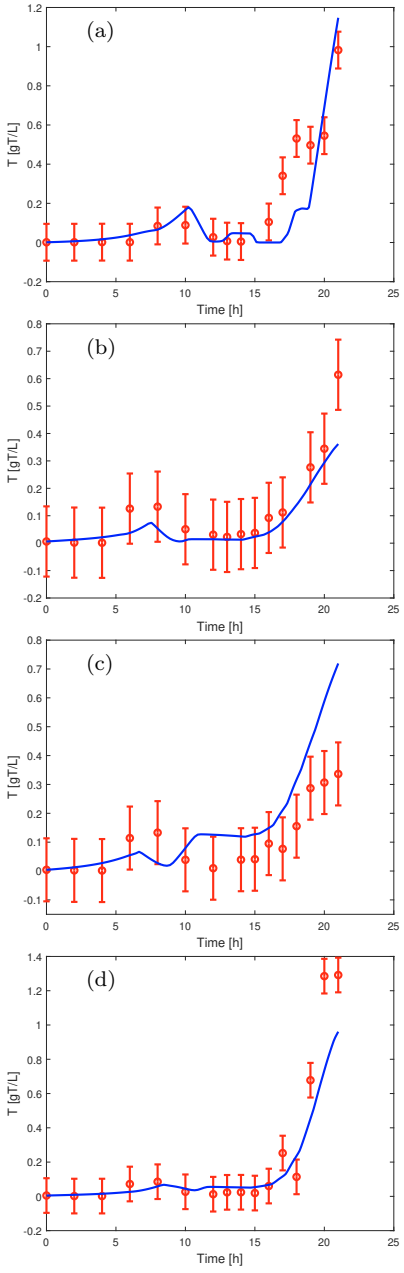

Fig. 4. Cross validation: predictions are obtained using the four sets of parameters estimated from data sets composed of three experiments. (a) Experiment 1 (Set 5), (b) Experiment 2 (Set 4), (c) Experiment 3 (Set 3), (d) Experiment 4 (Set 2)

Parapouli, M., Vasileiadis, A., Afendra, A.S., and Hatziloukas, E. (2020). *Saccharomyces cerevisiae* and its industrial applications. *AIMS Microbiol.*, 6, 1–31.

Richelle, A. and Bogaerts, Ph. (2014). Off-line optimization of baker's yeast production process. *Chem. Eng. Sci.*, 119, 40–52.

Richelle, A., Fickers, P., and Bogaerts, Ph. (2014). Macroscopic modelling of baker's yeast production in fed-batch cultures and its link with trehalose production. *Comput. Chem. Eng.*, 61, 220–233.

Saini, P., Beniwal, A., Kokkiligadda, A., and Vij, S. (2018). Response and tolerance of yeast to changing environmental stress during ethanol fermentation. *Process. Biochem.*, 72, 1–12.

Smallbone, K., Malys, N., Messiha, H., Wishart, J., and Simeonidis, E. (2011). Building a kinetic model of trehalose biosynthesis in *Saccharomyces cerevisiae*. *Method. Enzymol.*, 500, 355–370.

Sonnleitner, B. and Käppeli, O. (1986). Growth of *Saccharomyces cerevisiae* is controlled by its limited capacity: formulation and verification of a hypothesis. *Biotechnol. Bioeng.*, 28, 927–937.

Tapia, H. and Koshland, D. (2014). Trehalose is a versatile and long-lived chaperone for desiccation tolerance. *Curr. Biol.*, 24, 2758–2766.

Voit, E. (2003). Biochemical and genomic regulation of the trehalose cycle in yeast: review of observations and canonical model analysis. *J. Theor. Biol.*, 223, 55–78.